# Catalytic Activation of the Phosphatase MKP-3 by ERK2 Mitogen-Activated Protein Kinase

Montserrat Camps,* Anthony Nichols,* Corine Gillieron,* Bruno Antonsson,* Marco Muda,† Christian Chabert,* Ursula Boschert,* Steve Arkinstall*‡

MAP kinase phosphatase–3 (MKP-3) dephosphorylates phosphotyrosine and phosphothreonine and inactivates selectively ERK family mitogen-activated protein (MAP) kinases. MKP-3 was activated by direct binding to purified ERK2. Activation was independent of protein kinase activity and required binding of ERK2 to the noncatalytic amino-terminus of MKP-3. Neither the gain-of-function Sevenmaker ERK2 mutant D319N nor c-Jun amino-terminal kinase–stress-activated protein kinase (JNK/SAPK) or p38 MAP kinases bound MKP-3 or caused its catalytic activation. These kinases were also resistant to enzymatic inactivation by MKP-3. Another homologous but nonselective phosphatase, MKP-4, bound and was activated by ERK2, JNK/SAPK, and p38 MAP kinases. Catalytic activation of MAP kinase phosphatases through substrate binding may regulate MAP kinase activation by a large number of receptor systems.

Signal transduction pathways that lead to activation of MAP kinases control many diverse and essential functions in yeast, worms, flies, and mammals. Extracellular signal–regulated kinase-1 (ERK1) and ERK2 exemplify one class of MAP kinase that undergoes activation by a range of stimuli including growth factors, cytokines, cell adhesion, tumor-promoting phorbol esters, and oncogenes (*1*). Specific functions assigned to ERK activity include chemotaxis, neuronal differentiation, and synaptic changes underlying memory and learning, as well as cellular mitogenesis and oncogenic transformation (*1*, *2*).

Full activation of ERK requires phosphorylation of threonine and tyrosine residues by a class of MAP kinase/ERK kinase (MEK) exemplified by MEK-1 (*1*, *3*). Conversely, an emerging family of dual-specificity phosphatases that act on both phosphotyrosine and phosphothreonine reverse this process and also appear to be critical regulators of MAP kinase activity. CL100/3CH134 or MAP kinase phosphatase–1 (MKP-1) is the archetypal member of this gene family and has high substrate specificity for MAP kinases (*4*). Up to nine other mammalian dual-specificity phosphatases have been identified, and several of these are under tight transcriptional control and display distinct tissue, cell, and subcellular expression patterns (*5*, *6*). MKP-3 appears exceptional in that it specifically inactivates ERK as compared with c-Jun $NH_2$-terminal kinases/stress-activated protein kinases (JNK/SAPK) or p38 MAP kinases (*7*). We now show that ERK, but not other MAP kinases, cause substrate-triggered activation of MKP-3.

We purified various MKP-3 deletion mutants expressed in *Escherichia coli* and found that the $NH_2$-terminal noncatalytic domain (amino acids 1 to 221) binds tightly to its target MAP kinases p44 ERK1 and p42 ERK2 (*8*). Binding to purified ERK2 (*9*) stimulates *p*-nitrophenyl phosphate (*p*-NPP) phosphatase activity of full-length MKP-3 by up to 30-fold (Fig. 1A) (*10*). Both glutathione-S-transferase (GST)–ERK2 and ERK2 caused similar activation of either the fusion protein GST–MKP-3, His-tagged MKP-3, or free MKP-3 (*11*). Activation of MKP-3 was dose-dependent and saturable with half-maximal effect detected in the presence of 5 μg (~0.5 μM) of ERK2 (Fig. 1B). No increase in phosphatase activity was detected upon binding of ERK2 to a catalytically inactive MKP3 mutant in which Cys-293 is substituted by Ser (C293S) (Fig. 2, A and B). Consistent with ERK2 binding to MKP-3 through its $NH_2$-terminus (*8*), the purified MKP-3ΔN catalytic core (residues 153 to 381) was insensitive to enzymatic activation by ERK2 (Fig. 2C). Moreover, enzymatic activation of full-length MKP-3 by ERK2 was inhibited (half-maximal inhibition at ~ 1 μM) in the presence of the purified noncatalytic $NH_2$-terminus of MKP-3 (MKP-3ΔC; amino acids 1 to 221) (Fig. 2D). Addition of the catalytically inactive MKP-3 mutant C293S also inhibited ERK2-dependent activation of wild-type (WT) MKP-3 (Fig. 2D). Because both MKP-3ΔC and MKP-3 C293S bind ERK2 tightly (*8*), this inhibition probably reflects competition for ERK2 binding to WT MKP-3.

To examine whether ERK2 enzymatic activity is necessary for binding and catalytic activation of MKP-3, we purified an inactive GST-ERK2 mutant in which Lys-52 is changed to Ala (K52A) (*9*). Like WT MAP kinase, ERK2 K52A bound (*12*) to MKP-3 and increased phosphatase activity (Fig. 3, A and B). GST-ERK2 K52A did not phosphorylate myelin basic protein (MBP) (Fig. 3C), demonstrating that MKP-3 activation is independent of MAP kinase activity.

In both in vitro and in cell transfection studies, low concentrations of MKP-3 inactivate ERK but not JNK/SAPK or p38 MAP kinases (*7*), which also fail to bind directly to MKP-3 (Fig. 3A). Furthermore, activation of MKP-3 appears to be limited strictly to the ERK class of MAP kinase because neither SAPKα (JNK2), SAPKβ (JNK3), or p38 induced an increase in phosphatase activity (Fig. 3B). All MAP kinases tested appeared to be folded correctly and to be

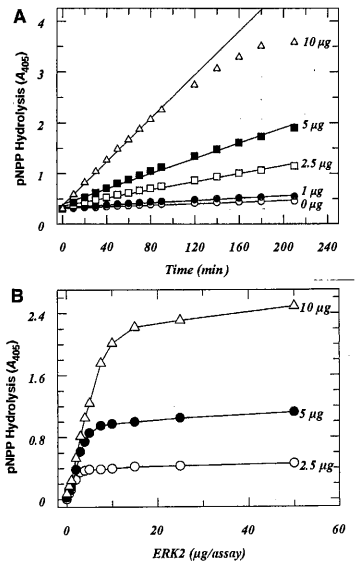


**Fig. 1.** Activation of MKP-3 by ERK2. Phosphatase activity was measured as *p*-NPP hydrolysis at 25°C monitored at an absorbance of 405 nm ($A_{405}$) (*10*). Full-length GST–MKP-3 and GST-ERK2 were expressed in *E. coli* and purified on glutathione-Sepharose. ERK2 was further purified by ion-exchange chromatography (*9*, *10*). (**A**) Time-dependent hydrolysis of *p*-NPP by 5 μg of GST–MKP-3 either alone (0 μg) or in the presence of the indicated amounts of ERK2. Linear reaction rates are indicated by lines of best fit. Ten micrograms of ERK2 stimulated phosphatase activity by 25.5-fold. (**B**) Activation of the indicated amounts of GST–MKP-3 by purified ERK2. Incubations were for 30 min. Maximal ERK2-dependent activation with 10 μg of MKP-3 was 35 times the basal phosphatase activity. Data points are the mean of duplicate determinations and are representative of three independent experiments.

Geneva Biomedical Research Institute, Glaxo Wellcome Research and Development S.A., CH-1228 Plan-les-Ouates, Geneva, Switzerland.

*Present address: Serono Pharmaceutical Research Institute, CH-1228, Plan-les-Ouates, Geneva, Switzerland. †Present Address: Department of Biological Chemistry, University of Michigan, Ann Arbor, MI 48109, USA. ‡To whom correspondence should be addressed. E-mail: steve.arkinstall@serono.com

active as indicated by phosphorylation of an appropriate substrate protein (9) (Fig. 3C) and activation of the MKP-3 homolog, MKP-4 (see below).

Genetic analysis in *Drosophila* suggests that the ERK MAP kinase *rolled* is a critical component of the Sevenless signal transduction pathway (*13*). A dominant gain-of-function mutation of the *rolled* MAP kinase gene, termed Sevenmaker, ($rl^{sevenmaker}$) contains a single amino acid substitution of Asn for Asp-334 (D334N) and activates several developmental pathways (*14*). The analogous mutant of mammalian ERK2 is also more sensitive to activation in vivo and appears to be resistant to inactivation by dual-specificity phosphatases in transfected cells (*15*). We tested the mammalian ERK2 Sevenmaker D319N mutation and found that it bound MKP-3 only weakly (Fig. 4A). Moreover, ERK2 D319N stimulated MKP-3 phosphatase activity only 10 to 15% as well as WT MAP kinase (Fig. 4B). This deficiency in its ability to trigger MKP-3 activation does not reflect misfolding of the purified Sevenmaker protein, which phosphorylated MBP as effectively as WT ERK2 (Fig. 4C). This observation suggests that one critical consequence of the ERK2 D319N mutation is an inability to bind and trigger catalytic activation of MKP-3.

To examine whether this deficiency is paralleled by resistance to inactivation, we next measured MKP-3–dependent inhibi-

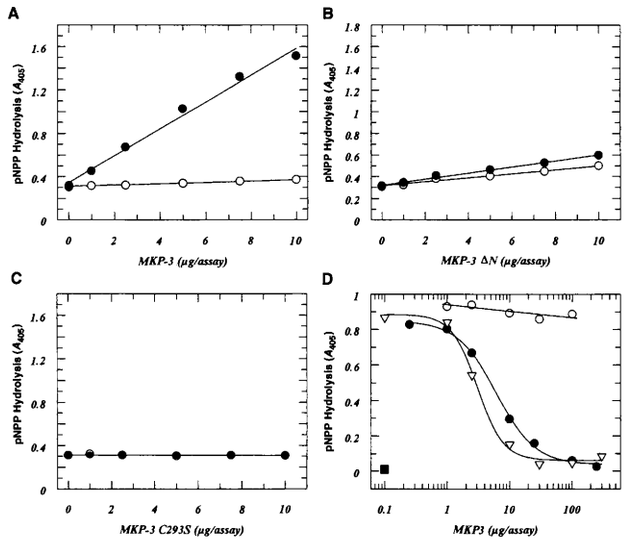


**Fig. 2.** Requirement of the MKP-3 catalytic Cys-293 and binding to the MKP-3 $NH_2$-terminus for ERK2-dependent activation. Phosphatase activity was measured as described (Fig. 1). Incubations were performed with the indicated concentrations of (**A**) WT GST–MKP-3, (**B**) inactive mutant GST–MKP-3 C293S, or (**C**) $NH_2$-terminally truncated GST–MKP-3ΔN (amino acids 153 to 381) in the absence (○) or presence (●) of ERK2 (5 μg). (**D**) Inhibition of ERK2-dependent activation of MKP-3 by the indicated concentrations of mutant inactive GST–MKP-3 (C293S) (▽), the MKP-3 $NH_2$-terminus GST-MKP-3ΔC (amino acids 1 to 221) (●), or GST protein (○) incubated in the presence of GST–MKP-3 (2.5 μg) and ERK2 (2.5 μg). (■) MKP-3 activity in the absence of ERK2. Data represent the mean of two identical experiments each performed in triplicate.

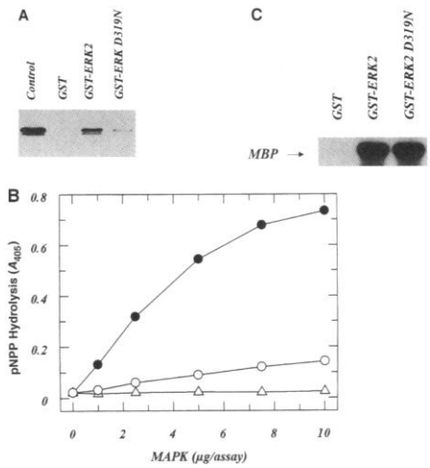


**Fig. 4.** Deficient binding and activation of MKP-3 by the ERK2 D319N Sevenmaker mutation. (**A**) GST-ERK2 or GST ERK2 D319N immobilized on glutathione-Sepharose beads (*9*) were incubated with His-tagged MKP-3, and binding was assessed as described (Fig. 3). His-tagged MKP-3 (7 ng) was used as a positive control. (**B**) Hydrolysis of *p*-NPP by MKP-3 in the presence of the indicated concentrations of GST-ERK2 (●), GST-ERK2 D319N Sevenmaker (○), or GST alone (△). (**C**) MBP phosphorylation by WT GST-ERK2 and Sevenmaker ERK2 D319N after incubation in kinase buffer in the presence of [γ -$^{32}$P]ATP (*9*). Proteins were separated and detected as described (Fig. 3).

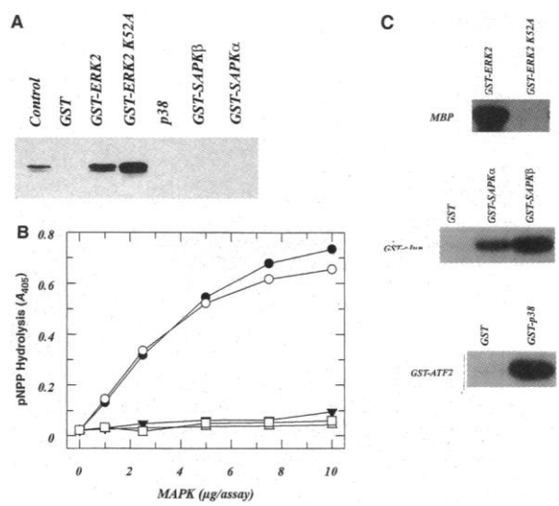


**Fig. 3.** ERK-specific binding and activation of MKP-3. (**A**) GST-ERK2, GST-ERK2K52A, GST-SAPKα (JNK2), GST-SAPKβ (JNK3), and GST-p38 MAP kinases immobilized on glutathione-Sepharose beads (*9*) were incubated with free His-tagged MKP-3 (*10*). After extensive washing, binding was assessed by protein immunoblotting. Bound MKP-3 was detected with a polyclonal antibody to MKP-3. Binding of antibody to rabbit immunoglobulin G coupled to peroxidase was detected by chemilumines-cence. His-tagged MKP-3 (5 ng) was used as a positive control. (**B**) Hydrolysis of *p*-NPP by MKP-3 in the presence of theindicated concentrations of eluted GST-ERK2 (○), catalytically inactive GST-ERK2 K52A (●), GST-SAPKα (JNK2) (▼), GST-SAPKβ (JNK3) (□), or GST-p38 MAP kinase (△). (**C**) Substrate phosphorylation by MAP kinase proteins used in (B). MAP kinases were incubated in kinase buffer in the presence of [γ -$^{32}$P]ATP (*9*) together with either MBP (GST-ERK2 or GST-ERK2 K52A), GST–c-Jun (1-79) [GST-SAPKα (JNK2) or GST-SAPKβ (JNK3)], or GST–ATF-2 (19-96) (GST-p38) before separation by SDS–polyacrylamide gel electrophoresis (15% gel), drying, and autoradiography. These experiments were performed three times with identical results.

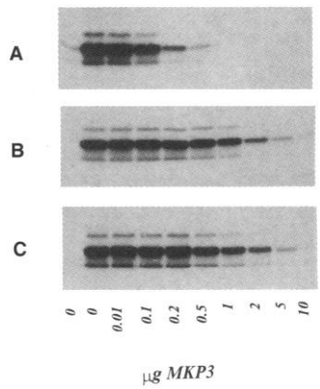


**Fig. 5.** Resistance of ERK2 D319N Sevenmaker to inactivation by MKP-3. Wild-type ERK2 (**A** and **C**) or ERK2 D319N (**B**) (0.5 μg) were incubated in vitro in the absence (lane 1) or presence (all other lanes) of 0.1 μg of constitutively active MEK1 (S217E S221E) (*16*) and with the indicated concentrations (0.01 to 10 μg) of full-length MKP-3 (A and B) or MKP-3ΔN (amino acids 153 to 381) (C). Figure shows autoradiograms of MBP phosphorylation by activated MAP kinases. Experiments were repeated three times with identical results.

tion of WT and Sevenmaker ERK2 activated in vitro by the constitutive MAP kinase kinase MEK1 in which Ser-217 and Ser-221 are changed to glutamate (S217E and S221E) (*16*). MKP-3 potently inactivated WT ERK2, but more than 10 times as much MKP-3 was required to inhibit MBP phosphorylation by the ERK2 Sevenmaker mutant (Fig. 5, A and B). Similar observations were also made in mammalian cells transfected with WT ERK2 or ERK2 D319N together with a range of MKP-3 plasmid concentrations (*17*). Epidermal growth factor (EGF)–stimulated ERK2 D319N activation was inhibited only partially at levels of MKP-3 expression that abolished WT ERK2 activity (Fig. 6A). Taken together, these observations indicate that the Sevenmaker mutation interferes with binding to MKP-3 and, as a consequence, prevents a substrate-dependent increase in MKP-3 phosphatase activity, resulting in less-effective ERK2 inactivation. Impaired catalytic activation of MKP-3 may thereby underlie the gain-of-function phenotype of the ERK2 Sevenmaker mutation.

These observations suggest that mutations in MKP-3 that interfere with binding to ERK2 may also lead to MAP kinase resistance to inactivation. Consistent with this prediction, the purified catalytic core of MKP-3 (MKP-3ΔN; amino acids 153 to 381), which failed to bind ERK2 (*8*) or to undergo enzymatic activation by this MAP kinase (Fig. 2C), was ~1/10th as effective at reversing in vitro ERK2 activation by MEK-1 (S217E and S221E) (Fig. 5C). Also in mammalian cells (*17*), EGF-stimulated ERK2 activity was resistant to inactivation by MKP-3ΔN as compared with WT MKP-3 (Fig. 6B). As anticipated by binding of ERK1 to the $NH_2$-terminus of MKP-3 (*8*), this closely related MAP kinase isoform was also resistant to inactivation by MKP-3ΔN in mammalian cells (Fig. 6C).

MKP-4 is a homologous dual-specificity phosphatase displaying low sequence identity with MKP-3 within its $NH_2$-terminus. MKP-4 also appears functionally distinct from MKP-3 in that it displays relatively nonselective inactivation of ERK, JNK/SAPK, and p38 MAP kinases (*6*). Consistent with these differences and unlike MKP-3, MKP-4 bound ERK2, SAPKβ (JNK3), and p38 and underwent dose-dependent *p*-NPP phosphatase activation by all three MAP kinase isoforms (Fig. 7, A and B). As with MKP-3, ERK2 D319N failed to bind or trigger catalytic activation of MKP-4 (*11*).

Transcription of many dual-specificity phosphatases is regulated in response to growth and differentiation factors or cell stresses (*4*–*6*). Our results indicate that their catalytic activation through binding substrate MAP kinases may represent a secondary posttranslational mechanism for control. ERK-specific MKP-3 activation through binding of its noncatalytic $NH_2$-terminus may indicate that sequence diversity of dual-specificity phosphatases within this region (*6*) enables their selective activation through binding different repertoires of substrate MAP kinases. This may provide a mechanism for targeted inactivation of selected MAP kinases.

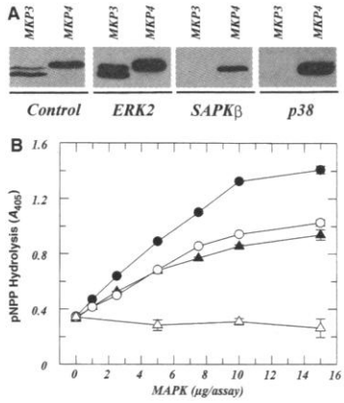


**Fig. 7.** MKP-4 binding and activation by ERK2, SAPKβ (JNK3), and p38 MAP kinases. (**A**) COS-7 cells transfected with Myc–MKP-3 or Myc–MKP-4 (*17*) were lysed and incubated with immobilized MAP kinases as described (Fig. 3). MKP-3 and MKP-4 bound to GST–ERK2, GST-SAPKβ (JNK3), and GST-p38 was measured by protein immunoblotting with monoclonal antibody to Myc (*12*). The control represents crude lysates from cells transfected as indicated. (**B**) Purified MKP-4 *p*-NPP phosphatase activity measured in the presence of the indicated concentrations of GST-ERK2 (●), GST-SAPKβ (JNK3) (▲), GST-p38 MAP (○), or GST (△). Data points are the mean of duplicate determinations and are representative of three independent experiments.

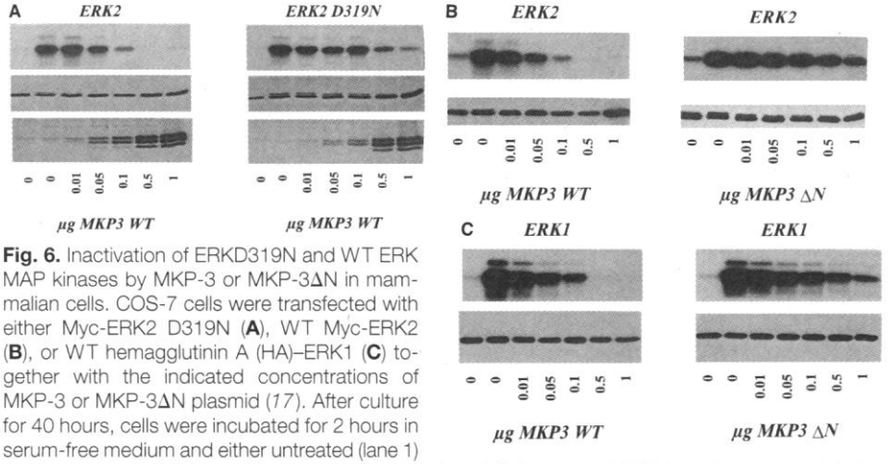


**Fig. 6.** Inactivation of ERKD319N and WT ERK MAP kinases by MKP-3 or MKP-3ΔN in mammalian cells. COS-7 cells were transfected with either Myc-ERK2 D319N (**A**), WT Myc-ERK2 (**B**), or WT hemagglutinin A (HA)–ERK1 (**C**) together with the indicated concentrations of MKP-3 or MKP-3ΔN plasmid (*17*). After culture for 40 hours, cells were incubated for 2 hours in serum-free medium and either untreated (lane 1) or stimulated with EGF (10 nM) for 10 min (all other lanes). Subsequent MAP kinase immunoprecipitation, immune complex assays, and protein immunoblotting were performed as described (*17*). (A) ERK2 D319N is resistant to inactivation by MKP-3 in COS-7 cells. (**Top**) Autoradiographs of MBP phosphorylation by EGF-stimulated ERK2 or ERK2 D319N in the absence and presence of various amounts of coexpressed WT MKP-3. (**Middle**) Protein immunoblotting of corresponding immunoprecipitated ERK2 or ERK2 D319N. (**Bottom**) Levels of immunodetected MKP-3 in crude cell lysates. (B and C) ERK2 and ERK1 are resistant to inactivation by MKP-3ΔN. (**Top**) Autoradiographs of MBP phosphorylation by EGF-stimulated ERK2 (B) or ERK1 (C) in the absence or presence of MKP-3 or MKP-3ΔN as indicated. (**Bottom**) Protein immunoblotting of corresponding immunoprecipitated ERK2 (B) or ERK1 (C). In (B) and (C), indistinguishable levels of MKP-3 and MKP-3ΔN protein expression were detected for each corresponding plasmid concentration (*11*). Each experiment was performed twice with identical results.

## REFERENCES AND NOTES


1. C. J. Marshall, *Cell* **80**, 179 (1995); J. E. Ferrell, *Curr. Top. Dev. Biol.* **33**, 1 (1996); P. Cohen, *Trends Cell Biol.* **7**, 353 (1997).
2. S. J. Mansour *et al.*, *Science* **265**, 966 (1994); S. Cowley, H. Paterson, P. Kemp, C. J. Marshall, *Cell* **77**, 841 (1994); D. T. Dudley *et al.*, *Proc. Natl. Acad. Sci. U.S.A.* **92**, 7686 (1995); J. M. Kornhauser and M. E. Greenberg, *Neuron* **18**, 839 (1997); A. A. Reszka, J. C. Bulinski, E. G. Krebs, E. H. Fischer, *Mol. Biol. Cell* **8**, 1219 (1997).
3. C. M. Crews, A. Alessandrini, R. L. Erikson, *Science* **258**, 478 (1992); J. Wu *et al.*, *Proc. Natl. Acad. Sci. U.S.A.* **90**, 173 (1993); C. H. Zheng and K. L. Guan, *J. Biol. Chem.* **268**, 11435 (1993).
4. H. Sun, C. H. Charles, L. F. Lau, N. K. Tonks, *Cell* **75**, 487 (1993); S. M. Keyse, *Biochim. Biophys. Acta* **1265**, 152, (1995).
5. A. Misra-Press, C. S. Rim, H. Yao, M. S. Roberson, P. J. S. Stork, *J. Biol. Chem.* **270**, 14587 (1995); S. P. Kwak and J. E. Dixon, *ibid.*, p. 1156; T. Ishibashi, D. P. Bottaro, P. Michieli, C. A. Kelley, S. A. Aaronson, *ibid.* **269**, 29897 (1994); K. J. Martell, A. F. Seasholtz, S. P. Kwak, K. K. Clemens, J. E. Dickson, *J. Neurochem.* **65**, 1823 (1995).
6. M. Muda *et al.*, *ibid.* **271**, 4319 (1996); M. Muda *et al.*, *ibid.* **272**, 5141 (1997).
7. M. Muda *et al.*, *ibid.* **271**, 27205 (1996); L. A. Groom, A. A. Sneddon, D. R. Alessi, S. Dowd, S. M. Keyse,

*EMBO J.* **15**, 3621 (1996).
8. M. Muda *et al.*, *ibid.* **273**, 9323 (1998).
9. ERK2, ERK2 K52A, ERK2 D319N, SAPKα (JNK2), SAPKβ (JNK3), and p38 MAP kinases were produced in *E. coli* as GST fusion proteins and purified by binding to glutathione-Sepharose. All MAP kinases were >90% pure. Bead-immobilized MAP kinases were used for binding MKP-3 (*13*); for phosphatase activation (*10*) MAP kinases were eluted with 50 mM tris (pH 8.0) containing 5 mM glutathione. For some experiments GST-ERK2 and GST–MKP-3 were cleaved from their GST fusion protein by incubation with thrombin and further purified by fast protein liquid chromatography with Mono Q Sepharose followed by dialysis against 20 mM tris (pH 7.5) containing 0.5 mM EGTA, 5 mM $MgCl_2$, and 2 mM dithiothreitol (DTT). This ERK2 was >95% pure. MAP kinase phosphorylation assays were done with [$\gamma$-$^{32}$P]ATP (adenosine 5′-triphosphate) as described (*6*, *8*).
10. MKP-3, catalytically inactive MKP-3 (C293S), MKP-3ΔN (amino acids 153 to 381), MKP-3ΔC (amino acids 1 to 221), and MKP-4 subcloned into pGEX 4T3 (*6*, *8*) were expressed in *E. coli* by induction with 100 μM isopropyl-β-D-thiogalactopyranoside and growth at 20°C. GST fusion proteins were purified with glutathione-Sepharose (Pharmacia LKB Biotechnology) and eluted in 50 mM tris (pH 8.0) containing 5 mM glutathione. His–MKP-3 was expressed under identical conditions and purified with Ni-agarose and eluted with 300 mM imidazole. All proteins were >90% pure. Phosphatase activity was measured in 96-well plates in 200 μl of 50 mM imidazole (pH 7.5) containing 5 mM DTT, 20 mM *p*-NPP, and the indicated concentrations of MKP-3 and various purified MAP kinases (*9*). Reaction rates were measured at 405 nm in a microplate reader (Molecular Devices).
11. M. Camps, C. Gillieron, S. Arkinstall, unpublished data.
12. His-tagged MKP-3 (0.1 μg) was incubated with MAP kinases immobilized on beads (3 μg) in 20 mM tris-acetate (pH 7.0) containing 1% Triton X-100, 50 mM NaF, 1 mM EDTA, 1 mM EGTA, 1 mM sodium vanadate, 0.27 M sucrose, 5 mM sodium pyrophosphate, 10 mM β-glycerophosphate, and 0.1% β-mercaptoethanol together with a cocktail of protease inhibitors overnight at 4°C with mixing. Beads were washed four times in 10 mM tris (pH 7.4), and bound MKP-3 was analyzed by protein immunoblotting with a polyclonal antibody directed to the peptide VVLYDENSSDWNENTGGE (amino acids 95 to 112). In some experiments COS-7 cells were transfected with pMT-SM-Myc-MKP-3 or pMT-SM-Myc-MKP-4 (*6*, *11*), and binding to immobilized MAP kinases (3 μg) was measured under identical conditions except that MKP-3 and MKP-4 protein was detected with monoclonal antibody to the Myc epitope (*8*). Abbreviations for the amino acid residues are as follows: D, Asp; E, Glu; G, Gly; L, Leu; N, Asn; S, Ser; T, Thr; V, Val; W, Trp; and Y, Tyr.
13. W. H. Biggs III and L. Zipursky, *Proc. Natl. Acad. Sci. U. S. A.* **89**, 6295 (1992); W. H. Biggs III *et al.*, *EMBO J.* **13**, 1628 (1994).
14. D. Brunner *et al.*, *Cell* **76**, 875 (1994).
15. C. M. Bott, S. G. Thorneycroft, C. J. Marshall, *FEBS Lett.* **352**, 201 (1994); Y. Chu, P. A. Solski, R. Khosravi-Far, C. J. Der, K. Kelly, *J. Biol. Chem.* **271**, 6497 (1996).
16. Constitutively active rabbit MEK1 EE (S217E and S221E) was purified and used to activate ERK as described (*8*).
17. COS-7 cells were transfected with pEXV3-Myc-ERK2, pEXV3-Myc-ERK2 D319N, or pcDNA1-HA-ERK1 together with various concentrations of pMT-SM-MKP-3 or pMT-SM-MKP-3ΔN followed by EGF stimulation, MAP kinase immunoprecipitation, and immune complex assays were performed exactly as described (*6*, *8*). pMT-SM-MKP-3ΔN (amino acids 153 to 381) was constructed by digesting pMT-SM-MKP-3 (*6*) with Pst I–Xba I followed by ligation with a double-stranded oligonucleotide containing an ATG codon following a Kozak consensus.
18. We thank J. R. Woodgett (Ontario Cancer Institute, Canada) for pMT2-HA-SAPKβ (JNK3) and pGEX-SAPKα (JNK2); E. Bettini (Glaxo Wellcome, Verona, Italy) for pGEX-c-Jun-(1-79); S. Stimpson (Glaxo Wellcome, Research Triangle Park, NC) for pGEX-p38; and C. J. Marshall (Chester Beatty Labs, ICR, London, UK) for pGEX-2T/ERK2, pGEX-2T/ERK2 D319N (Sevenmaker), pGEX-2T/ERK2 K52A, pGEX-3X/MEK1 (S217E, S221E), pEXV3-Myc-ERK2, pEXV3-Myc-ERK2 D319N, and rabbit antibody 122 specific for ERK2.

24 December 1997; accepted 9 April 1998

# Requirement for γδ T Cells in Allergic Airway Inflammation

Claudia Zuany-Amorim,* Claude Ruffié, Solomon Hailé, B. Boris Vargaftig, Pablo Pereira,† Marina Pretolani†‡

The factors that contribute to allergic asthma are unclear but the resulting condition is considered a consequence of a type-2 T helper ($T_H2$) cell response. In a model of pulmonary allergic inflammation, mice that lacked γδ T cells had decreases in specific immunoglobulin E (IgE) and IgG1 and pulmonary interleukin-5 (IL-5) release as well as in eosinophil and T cell infiltration compared with wild-type mice. These responses were restored by administration of IL-4 to γδ T cell-deficient mice during the primary immunization. Thus, γδ T cells are essential for inducing IL-4-dependent IgE and IgG1 responses and for $T_H2$-mediated airway inflammation to peptidic antigens.

Allergic asthma is a chronic inflammatory disease associated with a predominant $T_H2$ response, IgE synthesis, airway infiltration by inflammatory cells, particularly eosinophils, and bronchial hyperreactivity (*1*). Identification of the mechanisms involved in the in vivo commitment of naive T cells to a $T_H2$ phenotype will aid our understanding of the initiation and maintenance of tissue inflammation. IL-4 drives $T_H2$ responses and promotes IgE synthesis (*2*), but the nature of the cells that provide this cytokine after in vivo interactions among peptidic antigens, antigen-presenting cells, and $T_H$ cells remains largely elusive.

A subset of γδ T cells can produce $T_H2$-type cytokines (*3*, *4*) which suggests their possible participation in the development of $T_H2$ responses and, thus, in the onset of pulmonary allergic reactions. To address this question, we backcrossed 6-week-old mice that were genetically deficient in the δ chain of the T cell antigen receptor (TCR) and developed no γδ T cells (*5*) to BALB/c mice for 10 generations. These γδ T cell-deficient ($\gamma\delta^{-/-}$) and BALB/c wild-type ($\gamma\delta^{+/+}$) mice were repeatedly immunized intraperitoneally with soluble ovalbumin (OVA) and then challenged intranasally with OVA or saline (*6*). We analyzed airway infiltration by inflammatory cells (*7*), cytokine release in the bronchoalveolar lavage (BAL) fluid (*8*), bronchopulmonary hyperreactivity to inhaled methacholine (*9*), and OVA-specific IgE and IgG1 titers in the serum (*10*).

Repeated intranasal OVA challenges in immunized $\gamma\delta^{+/+}$ mice resulted in a significant increase in the number of eosinophils and of $CD4^+$ and $CD8^+$ T lymphocytes infiltrating the bronchial tissue (Fig. 1, A, D, and G). Eosinophils and T cells were located in the bronchial submucosa and around the blood vessels (Fig. 1, B, E, and H). Antigen-induced eosinophilia also occurred in the blood, BAL fluid, and bone marrow (*11*, *12*). Unlike $\gamma\delta^{+/+}$ mice, OVA-challenged $\gamma\delta^{-/-}$ mice showed only a moderate increase in the number of eosinophils in bronchial tissue, BAL fluid, blood, and bone marrow; no significant changes in T cell counts in lung tissue were observed (Fig. 1) (*12*).

Airway eosinophilia in OVA-challenged $\gamma\delta^{+/+}$ mice paralleled IL-5, but not interferon-γ (IFN-γ), production in the BAL fluid (Fig. 2), a finding consistent with selective induction of a $T_H2$ response in the airways. In contrast, $\gamma\delta^{-/-}$ mice failed to release IL-5 in response to intranasal administration of OVA (Fig. 2A) and the amounts of IFN-γ remained very low in both saline- and OVA-challenged animals (Fig. 2B). High concentrations of IL-4 were detected in the BAL fluid of saline-challenged $\gamma\delta^{+/+}$ and $\gamma\delta^{-/-}$ mice (445.6 ± 98.9 and 280.8 ± 42.9 pg/ml, respectively). These quantities decreased slightly after intranasal OVA challenge in

C. Zuany-Amorim, C. Ruffié, B. B. Vargaftig, M. Pretolani, Unité de Pharmacologie Cellulaire, Unité Associée Institut Pasteur/INSERM U485, Paris, France.
P. Pereira, Unité d'Immunobiologie, CNRS URA 1961, Institut Pasteur, Paris, France.
S. Hailé, Unité d'Histopathologie, Institut Pasteur, Paris, France.

*Present address: Novartis Horsham Research Centre, Horsham, UK.
†These authors contributed equally to this work.
‡To whom correspondence should be addressed. E-mail: mpretol@pasteur.fr